Journal of the Serbian Chemical Society
JSCS-info@shd.org.rs • www.shd.org.rs/JSCS

ACCEPTED MANUSCRIPT

Journal of the Serbian Chemical Society
JSCS-info@shd.org.rs • www.shd.org.rs/JSCS
J. Serb. Chem. Soc. **00(0)** 1-16 (2026)
JSCS–13941
Original scientific paper
Published DD MM, 2026

Investigation of the isomorphic substitution of P-V in the structure of calcium hydroxyapatite by X-ray and spectral methods

ELENA L. TIKHONOVA, TAISIYA D. BOLKHOVSKAYA, POLINA V. KORTIKOVA, AND EVGENY N. BULANOV*

Lobachevsky University, 23 Gagarin ave, Nizhny Novgorod, Russia, 603022.

(Received 1 May; revised 20 May; accepted 28 August 2026)

Abstract: The paper considers the possibility of forming a continuous series of solid solutions in the binary system $Ca_{10}(PO_4)_6(OH)_2$ - $Ca_{10}(VO_4)_6(OH)_2$, the extreme members of which belong to the structural type of apatite. The objects of the study were obtained by solid-phase reaction, the monophasicity of the products was confirmed by powder X-ray and IR spectroscopy. The detected anomalous deviations of the dependence of unit cell parameters on linearity (Vegard's rule) confirm the hypothesis of a possible ordering of phosphorus and vanadium atoms in solid solutions. The constancy of the volumetric coefficient of thermal expansion of the composition $Ca_{10}(PO_4)_3(VO_4)_3(OH)_2$ has been established with a change in temperature.

Keywords: apatite; isomorphism; phase analysis; IR spectroscopy; *in situ* thermo X-RAY diffraction.

INTRODUCTION

Materials based on stoichiometric synthetic calcium hydroxyapatite $Ca_{10}(PO_4)_6(OH)_2$ are currently considered as the basis for the creation of implants for bone restoration due to the crystallochemical identity of native bone.[1,2]

However, despite the proximity of the parameters of the structure and composition, such materials do not meet the requirements of resorbability after implantation.[3,4] In addition, there are a number of more general problems associated with the implantation of materials, such as the risk of periprosthetic infection. Currently, antibiotics added to the implant material or applied to the surgical site on a resorbable carrier are used to eliminate this risk factor.[5,6] This approach is also not without drawbacks – it is difficult to control the dosage of antibiotics and their toxic effect on the body.

To solve these problems, a number of scientific groups are developing approaches for chemical modification of the hydroxyapatite matrix to form

* Corresponding author. E-mail: bulanoven@chem.unn.ru
https://doi.org/10.2298/JSC260501053T

additional properties of the material, including increased strength, improved resorbability, antibacterial properties, *etc.*[7]

However, works focused on achieving specific properties, as a rule, have the disadvantage of lacking a theoretical foundation for the possibility of such modifications of compositions from the point of view of the crystallochemical features of the system, which leads to a phenomenological description of the results.[8,9]

In this paper, the theoretical and practical possibility of modifying synthetic hydroxyapatite with vanadium is considered as one of the most promising antimicrobial agents, including being a necessary ultramicroelement for the formation and normal functioning of solid tissues of the human body.[10] In addition, thermal deformations of the crystal structure during isomorphic P-V substitution have been studied, the results of which are necessary in the development of ceramic materials based on the solid solutions under consideration and modelling their behaviour at varying temperatures.

EXPERIMENTAL

Individual compounds of the compositions $Ca_{10}(PO_4)_6(OH)_2$ and $Ca_{10}(VO_4)_6(OH)_2$ were considered as the object of the study. The possibility of obtaining a continuous series of solid solutions of the composition $Ca_{10}(PO_4)_{6-x}(VO_4)_x(OH)_2$ was also studied (x = 0-6, step 1).

The synthesis of individual compounds and solid solutions was carried out by the solid phase reaction method according to the reaction scheme indicated below:

$$9Ca(NO_3)_2{\cdot}4H_2O + Ca(OH)_2 + (6\text{-}x)(NH_4)_2HPO_4 + xNH_4VO_4 \rightarrow$$
$$\rightarrow Ca_{10}(PO_4)_{6-x}(VO_4)_x(OH)_2 + \text{gaseous products}$$

The reagent mixture was weighed (analytical electronic scales BEL DA-723C, BEL ENGINEERING, weighing accuracy ± 0.001 g) in the required stoichiometric ratio, placed in a porcelain crucible and heated to a temperature of 150 °C, since calcium nitrate tetrahydrate begins to melt in its own water at a temperature of 42.7 °C and finally loses crystallization water at 132 °C, and the decomposition temperatures of ammonium metavanadate are 138 °C, and ammonium dihydrogen phosphate are 100-155 °C. Next, the temperature was raised at a rate of 25 degrees / hour to 600 °C, followed by exposure at 600 °C for 6 hours to decompose calcium nitrate. Further heat treatment involved stepwise heating to 1000 °C in increments of 100 degrees with exposure for 6-8 hours, dispersion in an agate mortar and control using X-ray diffraction at each stage. At a temperature of 1000 °C, the samples were calcined for 12 hours.

The proposed approach is based on our previous studies on the synthesis of solid solutions with an apatite-type structure, including those involving the substitution of phosphate ions by vanadate groups. [10–14] The periodic alternation of heating and grinding cycles helps to prevent the formation of secondary phases and to control the reaction rate. In essence, this constitutes a necessary condition for carrying out the synthesis of solid solutions under uniform conditions, since the end-member compositions are obtained at lower temperatures, whereas the intermediate compositions require higher temperatures. Therefore, the final synthesis temperature was chosen as the minimum temperature at which all of the investigated solid solutions can be obtained.

The chemical purity and elemental composition of the prepared samples were examined by energy-dispersive X-ray fluorescence analysis carried out in air on a long-wavelength dispersive X-ray fluorescence spectrometer (Shimadzu LAB CENTER XRF-1800). The quantification was performed using the fundamental parameters (FP) approach with a single certified reference material. The Kα emission line intensities were recorded in triplicate at an accelerating voltage of 40 kV and a tube current of 50 mA, employing a Rh anode, as well as flow proportional counter (FPC) and scintillation (SC) detectors.

X-ray phase analysis was performed using a Shimadzu XRD-6000 powder diffractometer (CuKa radiation, λ = 1.5406 Å, Bragg–Brentano focusing, 2θ = 10-60 °, scanning speed 2 deg/min). The Topas 3.0 software package was used for processing the results.[15] X-ray diffraction data of individual compounds $Ca_{10}(PO_4)_6(OH)_2$[16] (this model is a more general case of the hydroxyapatite structure, because the oxygen of the OH group is specified in position 4*e* rather than 2*a*/2*b*) and $Ca_{10}(VO_4)_6(OH)_2$,[17,18] with the apatite structure were used as models for phase analysis as well as other substances that can be formed in the system under consideration under the specified synthesis conditions (α-$Ca_2P_2O_7$,[19] β-$Ca_2P_2O_7$,[20] α-$Ca_3(PO_4)_3$,[21] β-$Ca_3(PO_4)_3$,[22] $Ca_3(VO_4)_3$[23]).

Scanning electron microscopy (SEM) in the secondary electron detection mode (Signal A = SE1) was used to obtain surface images of all compounds under study. Instrumental parameters: accelerating voltage 8.00 kV, probe current 2 pA. The SE1 mode provides high topographic contrast, which is ideally suited for examining the surface morphology of powder particles.

Determination of thermal expansion features of compounds under investigation realized using Shimadzu HA-1001 attachment (for the same diffractometer) in the range of 2θ angles from 10 to 60 ° with 100K step. Thermal expansion of compounds under study was analyzed using program complex ThetaToTensor 2.0.[24]

The IR spectra of the study objects were recorded on a Shimadzu FTIR Prestige–21 spectrometer (wavelength range 400 – 4000 cm^{-1}, signal accumulation – 20 scans) from suspensions in petroleum jelly placed between ZnSe plates. The assignment of vaseline bands was carried out using the AIST Spectral Database for Organic Compounds.[25]

RESULTS AND DISCUSSION

As it follows from Table I the composition of the resulting compounds was confirmed to be stoichiometric within a relative error of no more than 0.5%.

Table I. X-ray fluorescence analysis data for $Ca_{10}(PO_4)_{6-x}(VO_4)_x(OH)_2$ samples (x = 0-6).

	CaO, wt%		P_2O_5, wt%		V_2O_5, wt%	
x	calcld	found	calcld	found	calcld	found
0	55,8	55,8	42,4	42,4	0	0
1	54,7	54,7	34,6	34,6	8,9	8,8
2	53,7	53,6	27,2	27,2	17,4	17,5
3	52,7	52,7	20,0	20,1	25,6	25,6
4	51,7	51,8	13,1	13,0	33,5	33,5
5	50,8	50,7	6,4	6,2	41,2	41,1
6	49,9	49,9	0	0	48,5	48,6

According to the results of the X-ray diffraction analysis, the $Ca_{10}(PO_4)_6(OH)_2$ - $Ca_{10}(VO_4)_6(OH)_2$ system is characterized by the formation of a continuous series of solid solutions over the entire range of the studied compositions at temperatures above 1000 °C, as evidenced by the characteristic diffraction pattern of the structural type of apatite, which changes monotonously with changes in the composition of the object (Figure. 1). The observed shift of the diffraction maxima toward lower 2θ angles with increasing vanadium content is in full agreement with the previously established unit cell parameters for the individual compounds, [16–18] as well as with the Bragg–Wolff equation, which describes the inverse relationship between the interplanar spacing (and, consequently, the lattice parameters) and the diffraction angle.

The monophasicity of the obtained samples is confirmed not only by the absence of diffraction peaks impurity phases, but also the results of the analysis of IR spectra recorded after calcination of substances at 1000 °C (Figure 2-3).

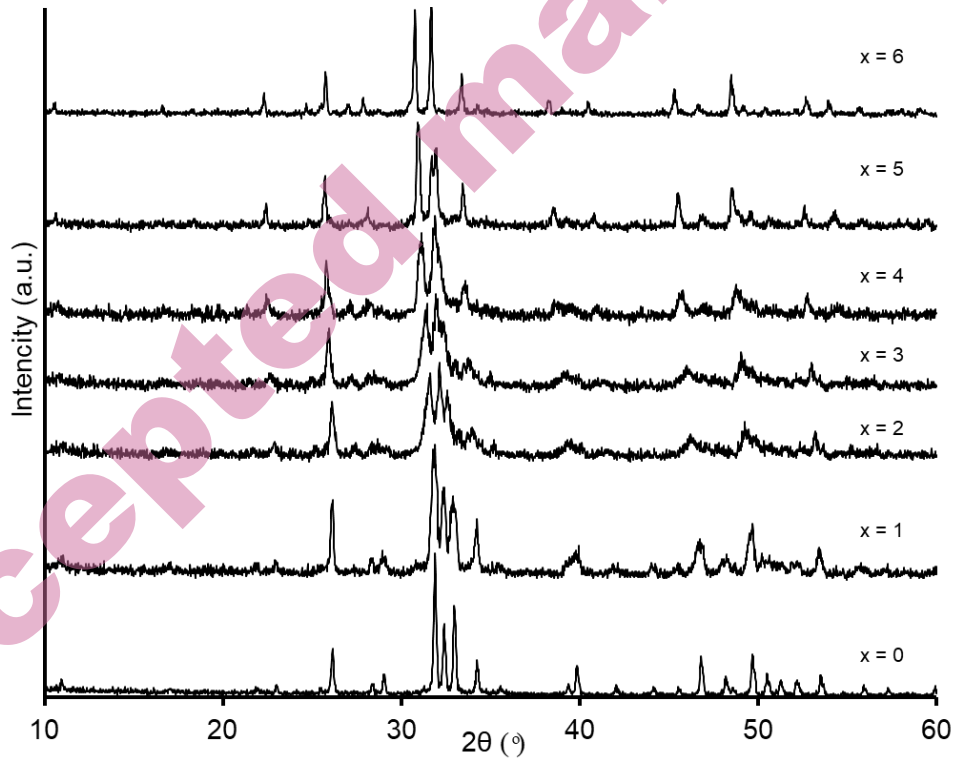

Fig. 1. XRD patterns of $Ca_{10}(PO_4)_{6-x}(VO_4)_x(OH)_2$ samples (x = 0-6) after calcination at 1000°C.

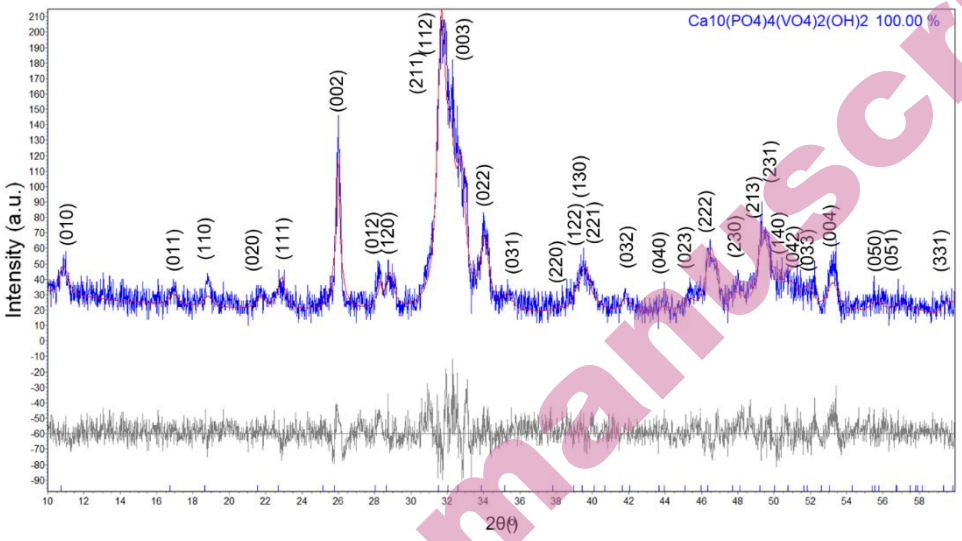

Fig. 2. X-ray phase analysis of the solid solution of composition $Ca_{10}(PO_4)_4(VO_4)_2(OH)_2$ with Miller indices assigned to the diffraction maxima of the apatite phase (blue – experimental diffraction pattern, red – simulated pattern, grey – difference pattern, blue triangles – positions of diffraction maxima).

Despite the presence of bands in the spectra in the ranges of 650-150 and 1300-1500 cm^{-1} wavenumbers due to the presence of petroleum jelly oil in the system, the identification of the main modes of the phosphate and vanadates under consideration can be carried out unambiguously. Thus, in the recorded spectra, the following are observed

- stretching modes of slightly distorted phosphate tetrahedra (v (PO_4^{3-})) in the range of wavenumbers 900-1150 cm^{-1},
- deformation modes of phosphate tetrahedra (δ (PO_4^{3-})) in the range of wavenumbers 500-150 cm^{-1},
- stretching modes of vanadium tetrahedra (v (VO_4^{3-})) in the range of wavenumbers 750 – 930 cm^{-1}.

The bands of deformation modes of vanadium tetrahedra are not visible, since they are outside the range of operation of the used spectrometer (below 400 cm^{-1}).[26] At the same time, bands of pyrophosphate ($P_2O_7^{4-}$)[27] and pyrovanadate groups ($V_2O_7^{4-}$)[28] are not observed.

The morphology of a powdered sample was investigated using SEM at a magnification of ×5 000. All samples under study were found to consist of polydisperse, irregularly shaped particles, predominantly in the size range of 0.5 to 7 μm, with a tendency to form loose agglomerates. The particle surfaces display pronounced micro-roughness, indicative of a high specific surface area. The

uniform contrast and the absence of bright inclusions suggest compositional homogeneity (Figure 4).

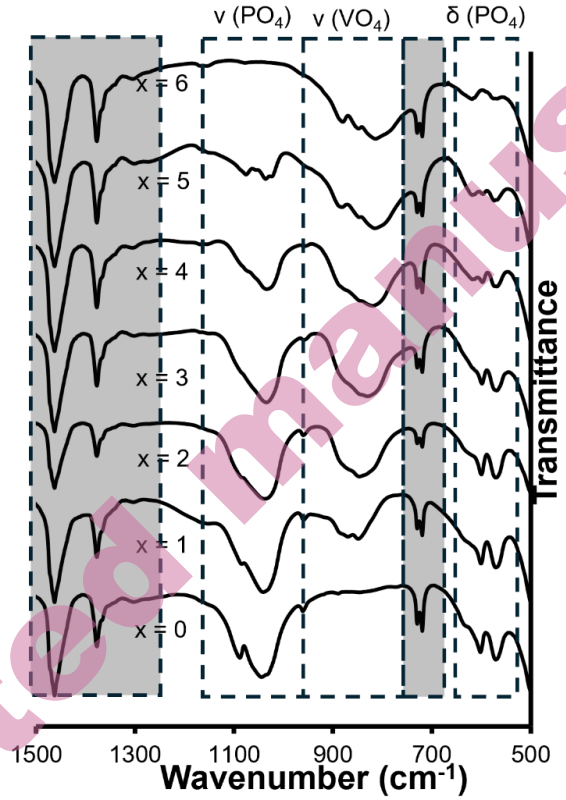

Fig.3. IR spectra of $Ca_{10}(PO_4)_{6-x}(VO_4)_x(OH)_2$ samples (x = 0-6) (gray colour indicates the areas of vibrations of the functional groups of petroleum jelly).

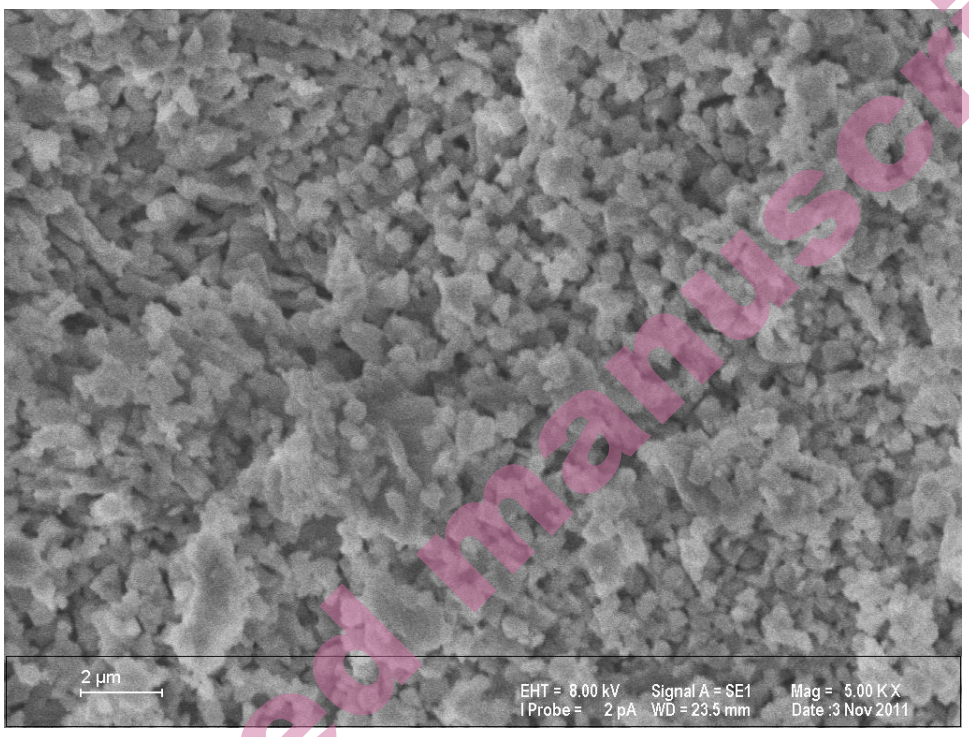

Fig. 4. Typical scanning electron microscopy (SEM) image of the powdered sample of $Ca_{10}(PO_4)_3(VO_4)_3(OH)_2$ (SE1 mode, ×5 000, scale bar 2 µm).

Based on the analytical indexing of powder XRD-patterns, the dependences of the parameters of the unit cells of the objects of study on the composition were calculated.

As can be seen from Figure 5, deviations from both the Vegard rule and the Retgers rule are observed in this system.

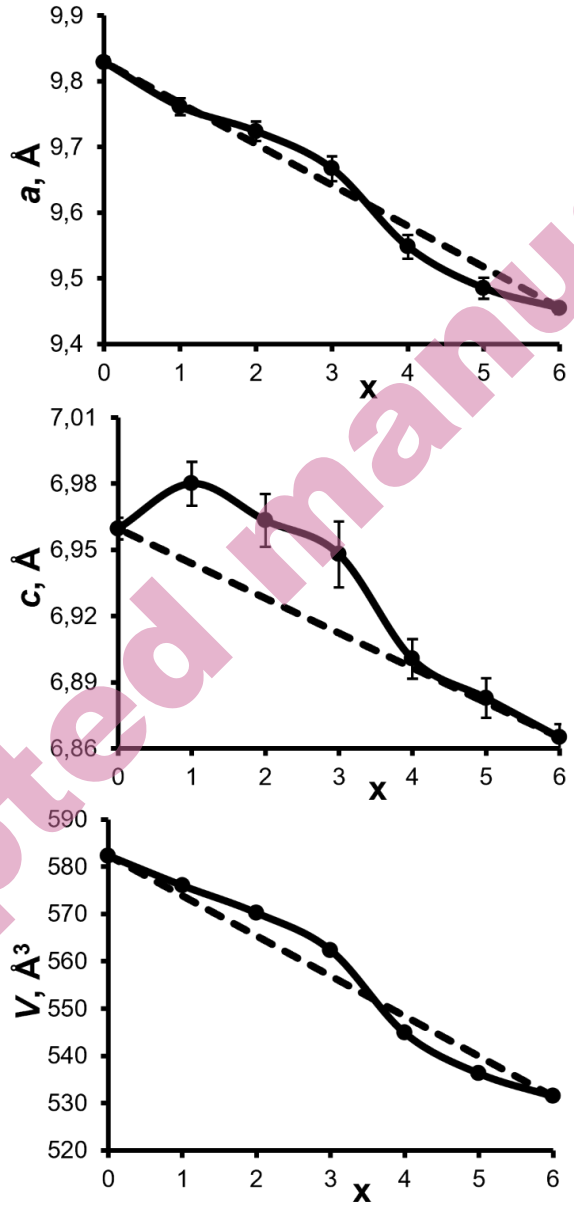

Fig.5. Dependences of the unit-cell parameters of the of samples $Ca_{10}(PO_4)_{6-x}(VO_4)_x(OH)_2$ (x = 0-6, step 1) on the composition (the dotted line shows the theoretical dependencies in accordance with the rules of Vegard and Retgers).

Positive deviations from the empirical rules of isomorphism are observed for compositions $0 < x < 3$, i.e., when phosphate ions are introduced into the calcium hydroxyvanadate matrix. A similar situation was observed with the substitution of

phosphate and vanadium ions in the structure of $Pb_{10}(AO_4)_6Cl_2$.[11] Subsequently, this apparent contradiction to the Goldschmidt-Fersman principle of directed substitution[29] was hypothetically explained by the ordering of phosphate and vanadium tetrahedra, indirectly experimentally confirmed by the anomalous thermal expansion of a solid solution of the composition $Pb_{10}(PO_4)_3(VO_4)_3Cl_2$.[30]

The minimal deviations from linearity in the dependences for parameters *a* and *V* indicate that atomic substitutions in the tetrahedral position of the crystal structure of apatite (even at $\Delta r/r = 1$ for phosphorus and vanadium)[31,32] do not affect the size of atomic layers perpendicular to the direction *c* (Figure 6), which is determined in this structural type exclusively by the cationic sublattice.

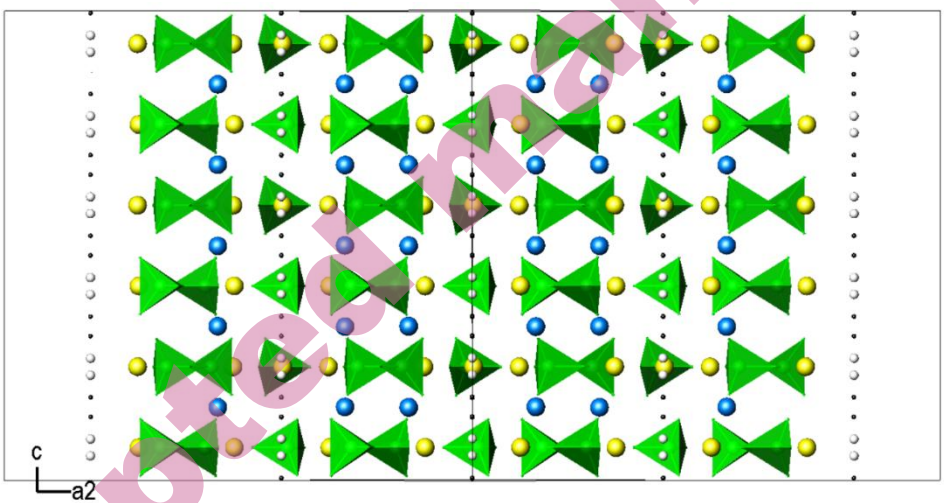

Fig. 6. Fragment of the crystal structure of $Ca_{10}(PO_4)_6(OH)_2$: the blue spheres are Ca cations at 4*f* position, the yellow ones are Ca cations at 6*h* position, the white ones are oxygens of hydroxyl groups, and the black ones are hydrogens of hydroxyl groups. Orthophosphate groups are represented as polyhedra.

The study of thermal deformations of the crystal structure of synthesized solid solutions also confirms the hypothesis of the ordering of tetrahedral groups PO_4 and VO_4 (Table II, Figure 7). The typical values and linear dependences of the volumetric coefficients of thermal expansion[33,34] for the extreme terms of the series degenerate into a constant α_V with a temperature change in the composition $Ca_{10}(PO_4)_3(VO_4)_3(OH)_2$.

Table II. Thermal dependencies of unit-cell parameters and linear and volumetric thermal expansion coefficients for apatites under study

T (K)	a (Å)	α_a (K^{-1})·10^6	c (Å)	α_c (K^{-1})·10^6	V (Å^3)	α_V (K^{-1})·10^6
			x=0			
298	9.829(1)	7.1(5)	6.9596(8)	10.3(9)	582.2(1)	24.4(1)
373	9.836(1)	8.6(4)	6.967(1)	12.4(7)	583.7(1)	29.5(9)
473	9.843(1)	10.6(3)	6.978(1)	15.1(5)	585.4(1)	36.4(6)
573	9.856(1)	12.7(2)	6.989(1)	17.8(4)	587.9(1)	43.1(4)
673	9.868(2)	14.7(1)	7.001(2)	20.5(3)	590.4(2)	49.9(3)
773	9.886(2)	16.7(2)	7.016(2)	23.2(3)	593.8(2)	56.6(4)
873	9.903(2)	18.7(3)	7.032(2)	25.8(5)	597.2(2)	63.3(6)
973	9.922(2)	20.7(4)	7.053(2)	28.5(7)	601.3(2)	70.0(8)
1073	9.943(3)	22.7(5)	7.075(3)	31.1(9)	605.7(3)	76.6(1)
			x=1			
298	9.7613(8)	7.9(8)	6.980(1)	8.8(5)	575.9(1)	24.6(2)
373	9.768(1)	9.4(6)	6.985(1)	10.3(4)	577.1(1)	29.2(1)
473	9.777(1)	11.5(5)	6.991(1)	12.3(3)	578.7(1)	25.4(1)
573	9.787(1)	13.6(6)	7.00(1)2	14.3(2)	580.8(1)	41.5(7)
673	9.805(2)	15.7(2)	7.013(2)	16.2(1)	583.8(2)	47.7(5)
773	9.822(2)	17.8(3)	7.025(2)	18.2(2)	586.9(2)	53.8(6)
873	9.839(2)	19.9(4)	7.038(2)	20.1(3)	590.0(2)	59.8(7)
973	9.861(3)	21.9(6)	7.053(3)	22.1(4)	593.9(3)	65.9(1)
1073	9.881(3)	23.9(7)	7.069(3)	24.0(5)	597.7(3)	71.8(3)
			x=2			
298	9.7239(8)	5.9(8)	6.9633(9)	6.4(6)	570.1(1)	18.1(2)
373	9.729(1)	7.2(6)	6.968(1)	7.9(6)	571.1(1)	22.3(2)
473	9.738(1)	9.0(5)	6.974(1)	9.8(4)	572.7(1)	27.7(2)
573	9.745(1)	10.7(3)	6.980(1)	11.8(3)	574.0(1)	33.2(6)
673	9.756(2)	12.5(2)	6.991(2)	13.7(2)	576.2(2)	38.6(5)
773	9.770(2)	14.2(3)	6.999(2)	15.6(2)	578.5(2)	44.1(7)
873	9.788(2)	16.0(4)	7.013(2)	17.6(4)	581.8(2)	49.5(3)
973	9.802	17.7(6)	7.025(3)	19.5(5)	584.5(3)	54.8(4)
1073	9.819(3)	19.4(7)	7.039(3)	21.3(6)	587.7(3)	60.2(5)
			x=3			
298	9.667(1)		6.948(1)		562.3(1)	
373	9.684(1)		6.951(1)		564.5(1)	
473	9.701(1)		6.95(1)		566.8(1)	
573	9.718(1)		6.958(1)		569.1(1)	
673	9.735(2)	18.0(2)	6.962(2)	6.2(5)	571.4(2)	41.1(4)
773	9.752(2)		6.9655(2)		573.7(2)	
873	9.769(2)		6.969(2)		575.9(2)	
973	9.786(3)		6.972(3)		578.2(3)	
1073	9.803(3)		6.976(3)		580.5(3)	

Table II. continued

T (K)	a (Å)	α_a (K^{-1})·10^6	c (Å)	α_c (K^{-1})·10^6	V (Å^3)	α_V (K^{-1})·10^6
			x=4			
298	9.5482(8)	6.3(6)	6.9006(9)	7.9(6)	544.8(1)	20.5(4)
373	9.552(1)	7.8(6)	6.905(1)	9.2(5)	545.6(1)	24.8(2)
473	9.560(1)	9.7(4)	6.913(1)	10.9(3)	547.1(1)	30.4(6)
573	9.571(1)	11.7(3)	6.919(1)	12.6(2)	548.8(1)	35.9(6)
673	9.582(2)	13.6(2)	6.929(2)	14.3(2)	550.9(2)	41.5(4)
773	9.599(2)	15.5(2)	6.941(2)	16.0(2)	553.8(2)	47.1(5)
873	9.612(2)	17.4(4)	6.952(2)	17.7(3)	556.2(2)	52.6(8)
973	9.632(3)	19.3(5)	6.964(3)	19.4(5)	559.5(3)	58.0(3)
1073	9.649(3)	21.2(6)	6.979(3)	21.2(5)	562.7(3)	63.5(4)
			x=5			
298	9.4852(9)	4.9(7)	6.8829(9)	5.8(2)	536.2(1)	15.6(3)
373	9.489(1)	6.9(6)	6.888(1)	8.0(2)	537.1(1)	21.8(2)
473	9.498(1)	9.5(4)	6.892(1)	11.0(2)	538.4(1)	30.0(2)
573	9.505(1)	12.1(3)	6.899(1)	13.9(6)	539.7(1)	38.2(3)
673	9.521(2)	14.7(2)	6.910(2)	16.8(5)	542.4(2)	46.3(5)
773	9.535(2)	17.3(3)	6.925(2)	19.8(6)	545.2(2)	54.4(4)
873	9.553(2)	19.9(4)	6.943(2)	22.7(7)	548.7(2)	62.5(2)
973	9.575(3)	22.5(5)	6.958(3)	25.5(2)	552.4(3)	70.5(2)
1073	9.595(3)	25.1(7)	6.972(3)	28.4(4)	555.8(3)	78.5(3)
			x=6			
298	9.454(1)	10.7(6)	6.865(1)	7.0(6)	531.4(1)	28.5(2)
373	9.462(1)	11.4(6)	6.866(1)	8.0(5)	532.5(1)	30.7(2)
473	9.471(1)	12.2(4)	6.874(1)	9.3(4)	534.0(1)	33.6(7)
573	9.486(1)	13.0(3)	6.880(1)	10.5(3)	536.2(1)	36.5(5)
673	9.500(2)	13.8(2)	6.889(2)	11.8(2)	538.4(2)	39.4(4)
773	9.510(2)	14.6(3)	6.898(2)	13.1(3)	540.3(2)	42.3(5)
873	9.525(2)	15.4(4)	6.906(2)	14.3(4)	542.7(2)	45.2(7)
973	9.541(3)	16.2(5)	6.915(3)	15.5(4)	545.2(3)	48.0(2)
1073	9.557(3)	17.0(6)	6.928(3)	16.8(6)	548.1(3)	50.9(2)

Possible variants of the structure ordering are shown in Figure 8. Option **a**, similar to the result of the "order-disorder" transition in the Cu-Au alloy,[35] seems less likely, as does option **b**. In the case of variant **c**, a tetrahedron vanadate layer "isolated" from phosphate arises, which, due to the greater deformability of the electron shell of vanadium atoms compared to phosphorus, will ensure not only the stability of volumetric thermal expansion, but also the predominance of expansion along the crystallographic direction *a* compared to the direction *c*, which is typical for purely vanadic apatites.

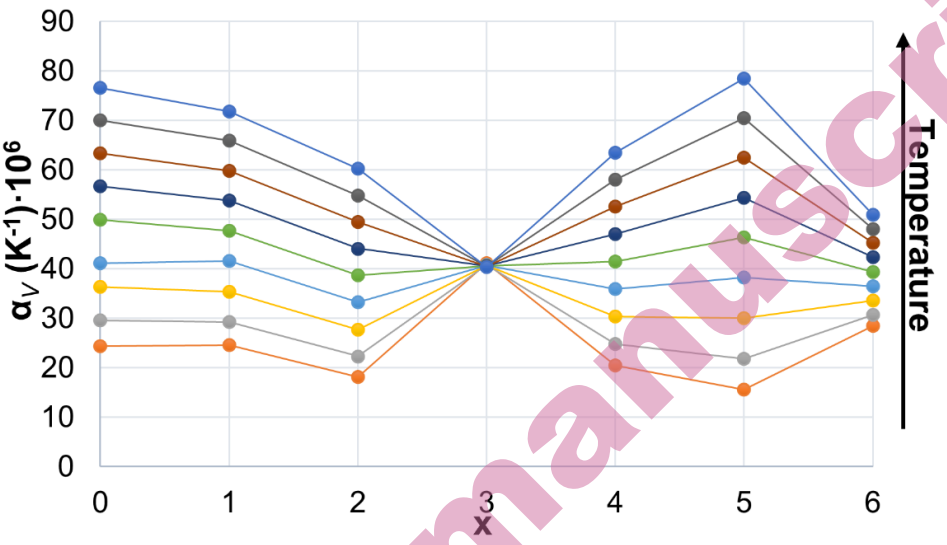

Fig.7. Thermal dependencies of volume thermal expansion coefficient for $Ca_{10}(PO_4)_{6-x}(VO_4)_x(OH)_2$ solid solutions

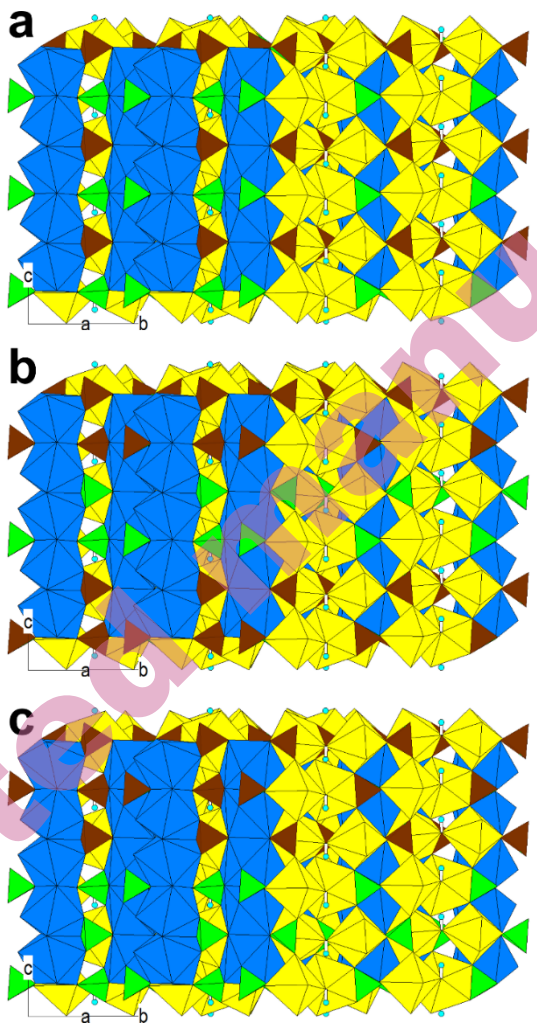

Fig. 8. Possible ordering options for phosphate (green) and vanadium (brown) tetrahedra in the crystalline structure of $Ca_{10}(PO_4)_3(VO_4)_3(OH)_2$ solid solution

CONCLUSION

Thus, when considering the possibility of forming solid solutions in the binary system $Ca_{10}(PO_4)_6(OH)_2$ - $Ca_{10}(VO_4)_6(OH)_2$ it has been established that a continuous series of phases of variable composition can be formed, despite the contradiction to the empirical rules of isomorphism (Goldschmidt's rule of 15% difference in radii of substituted atoms). This result indicates the importance of considering isomorphic substitutions without taking into account the structural type and layout features of a particular crystal lattice.

In turn, the established continuous substitution of vanadium for phosphorus in the hydroxyapatite structure makes it possible to develop biomaterials based on substances of the chemical compositions under consideration with controlled, i.e. a priori set properties.

The features of thermal deformations of the crystal structure associated with the possible ordering of isomorphically replaceable structural units make it possible to control the sintering processes of ceramic materials, avoiding the accumulation of stresses in the structure and, as a result, cracking of the material at the manufacturing stage.

Acknowledgements: The research was carried out with financial support via State assignment in Research scientific laboratory of "Chemistry of natural products and their synthetic analogues", grant number FSWR-2024-0002. The authors express their sincere gratitude to the Candidate of Chemical Sciences, Assoc. Permin D.A., graduate student Krasnov M.V. for their help in conducting experiments.

И З В О Д

ИСПИТИВАЊЕ ИЗОМОРФНЕ P–V СУПСТИТУЦИЈЕ У СТРУКТУРИ КАЛЦИЈУМ-ХИДРОКСИАПАТИТА ПРИМЕНОМ РЕНДГЕНСКИХ И СПЕКТРАЛНИХ МЕТОДА

ELENA L. TIKHONOVA, TAISIYA D. BOLKHOVSKAYA, POLINA V. KORTIKOVA, И EVGENY N. BULANOV*

Lobachevsky University, 23 Gagarin ave, Nizhny Novgorod, Russia, 603022.

У раду је размотрена могућност формирања континуираног низа чврстих раствора у бинарном систему $Ca_{10}(PO_4)_6(OH)_2$ - $Ca_{10}(VO_4)_6(OH)_2$, чији крајњи чланови припадају структурном типу апатита. Испитивани узорци добијени су реакцијом у чврстој фази, а једнофазност производа потврђена је рендгенском дифракцијом на праху и IR спектроскопијом. Уочена аномална одступања зависности параметара јединичне ћелије од линеарности (Вегардовог правила) потврђују претпоставку о могућем уређењу атома фосфора и ванадијума у чврстим растворима. Утврђена је константност запреминског коефицијента термичког ширења састава $Ca_{10}(PO_4)_3(VO_4)_3(OH)_2$ при промени температуре.

(Примљено 1. маја; ревидирано 20. маја; прихваћено 28. августа 2026.)

REFERENCES

1. S. V. Dorozhkin, *J. Compos. Sci.* **8** (2024) 218 (https://doi.org/10.3390/jcs8060218)
2. T. H. M. Mysore, A. Y. Patil, C. Hegde, M. A. Sudeept, R. Kumar, M. E. M. Soudagar, I. M. R. Fattah, *Eur. Polym. J.* **209** (2024) 112842 (https://doi.org/10.1016/j.eurpolymj.2024.112842)
3. T. J. Webster, E. A. Massa-Schlueter, J. L. Smith, E. B. Slamovich, *Biomaterials* **25** (2004) 2111–2121 (https://doi.org/10.1016/j.biomaterials.2003.09.001)
4. S. Sumathi, B. Gopal, *J. Cryst. Growth* **422** (2015) 36–43 (https://doi.org/10.1016/j.jcrysgro.2015.04.022)
5. L. Oezel, C. Büren, A. O. Scholz, J. Windolf, C. D. Windolf, *PLoS One* **14** (2019) e0213590 (https://doi.org/10.1371/journal.pone.0213590)
6. I. Karacan, B. Ben-Nissan, J. Santos, S. Yiu, P. Bradbury, S. M. Valenzuela, J. Chou, *J. Tissue Eng. Regen. Med.* **16** (2022) 1149–1162 (https://doi.org/10.1002/term.3353)
7. S. Shanmugam, B. Gopal, *Appl. Surf. Sci.* **303** (2014) 277–281 (https://doi.org/10.1016/j.apsusc.2014.02.166)
8. S. Sumathi, B. Gopal, *Ceram. Int.* **41** (2015) 4852–4860 (https://doi.org/10.1016/j.ceramint.2014.12.043)
9. E. N. Bulanov, O. N. Golitsyna, Y. V. Ostrovskaya, M. N. Egorikhina, M. I. Zaslavskaya, D. Y. Aleynik, *Ceram. Int.* **50** (2024) 11150–11157 (https://doi.org/10.1016/j.ceramint.2024.01.016)
10. E. N. Bulanov, K. S. Stasenko, M. N. Egorikhina, M. I. Zaslavskaya, D. Y. Aleynik, *Solid State Sci.* **151** (2024) Article number 107527 (https://doi.org/10.1016/j.solidstatesciences.2024.107527)
11. N. G. Chernorukov, A. V. Knyazev, E. N. Bulanov, *Russ. J. Inorg. Chem.* **55** (2010) 1463–1470 (https://doi.org/10.1134/S0036023610090226)
12. A. V Knyazev, N. G. Chernorukov, E. N. Bulanov, *Thermochim. Acta* **513** (2011) 112–118 (https://doi.org/10.1016/j.tca.2010.11.020)
13. A. V. Knyazev, N. G. Chernorukov, E. N. Bulanov, *Thermochim. Acta* **526** (2011) 72–77 (https://doi.org/10.1016/j.tca.2011.08.028)
14. E. N. Bulanov, A. A. Vasileva, S. A. Kazakovtsev, O. N. Golitsyna, E. V. Syrov, A. V. Knyazev, *Ceram. Int.* **49** (2023) 34097–34104 (https://doi.org/10.1016/j.ceramint.2023.08.113)
15. A. A. Coelho, *J. Appl. Crystallogr.* **51** (2018) 210–218 (https://doi.org/10.1107/S1600576718000183)
16. A. T. Sänger, W. F. Kuhs, *Zeitschrift fur Krist.* **199** (1992) 123–148 (https://doi.org/10.1524/ZKRI.1992.199.1-2.123)
17. A. Kutoglu, *Neues Jahrb. fuer Mineral.* **1974** (1974) 210–218 (https://doi.org/10.1127/njmm/1974/1974/210)
18. C. B. Boechat, J.-G. Eon, A. M. Rossi, C. A. de Castro Perez, R. A. da Silva San Gil, *Phys. Chem. Chem. Phys.* **2** (2000) 4225–4230 (https://doi.org/10.1039/B004339G)
19. C. Calvo, *Inorg. Chem.* **7** (1968) 1345–1351 (https://doi.org/10.1021/ic50065a019)
20. N. C. Webb, *Acta Crystallogr.* **21** (1966) 942–948 (https://doi.org/10.1107/s0365110x66004225)
21. R. M. Thompson, X. Xie, S. Zhai, R. T. Downs, H. Yang, *Am. Mineral.* **98** (2013) 1585–1592 (https://doi.org/10.2138/am.2013.4435)
22. P. A. Henning, E. Adolfsson, J. Grins, *Zeitschrift fuer Krist.* **215** (2000) 226–230 (https://doi.org/10.1524/zkri.2000.215.4.226)

23. R. Gopal, C. Calvo, *Zeitschrift fuer Krist. Crist. Mat.* **137** (1973) 67–85 (https://doi.org/10.1524/zkri.1973.137.16.67)
24. R. S. Bubnova, V. A. Firsova, S. K. Filatov, *Glas. Phys. Chem.* **39** (2013) 347–350 (https://doi.org/10.1134/S108765961303005X)
25. AIST Spectral Database for Organic Compounds, https://sdbs.db.aist.go.jp/ (accessed: May 1, 2026)
26. K. Nakamoto, *Infrared and Raman Spectra of Inorganic and Coordination Compounds*, Fourth Edi Jhn Wiley and Sons, Inc, New York, 1986
27. G. Buvaneswari, U. V. Varadaraju, *J. Solid State Chem.* **149** (2000) 133–136 (https://doi.org/10.1006/jssc.1999.8510)
28. I. E. Glazov, V. K. Krut'ko, O. N. Musskaya, A. I. Kulak, *Russ. J. Inorg. Chemsitry* **67** (2022) 173–182 (https://doi.org/10.1134/S0036023622020048)
29. V. S. Urusov, *Theoratical crystall chemistry*, 1987
30. A. V. Knyazev, E. N. Bulanov, V. Z. Korokin, *Mater. Res. Bull.* **61** (2014) 47–53 (https://doi.org/10.1016/j.materresbull.2014.09.089)
31. R. D. Shannon, *Acta Crystallogr. Sect. A.* **32** (1976) 751-767 (https://doi.org/10.1107/S0567739476001551)
32. Database of Ionic Radii, http://abulafia.mt.ic.ac.uk/shannon/ptable.php (accessed: November 27, 2025)
33. N. G. Chernorukov, A. V. Knyazev, E. N. Bulanov, *Inorg. Mater.* **47** (2011) 172 (https://doi.org/10.1134/S002016851101002X)
34. A. V. Knyazev, N. G. Chernorukov, E. N. Bulanov, *Mater. Chem. Phys.* **132** (2012) (https://doi.org/10.1016/j.matchemphys.2011.12.011)
35. A. V. Glukhov, V. A. Kazantsev, A. Y. Volkov, B. D. Antonov, *Tech. Phys.* **65** (2020) 87–92 (https://doi.org/10.1134/S1063784220010065).